Journal of Magnetic Resonance **140,** 259–263 (1999)
Article ID jmre.1999.1820, available online at http://www.idealibrary.com on IDEAL®

COMMUNICATIONS

Pulse Sequences for Measurement of One-Bond ^{15}N–^{1}H Coupling Constants in the Protein Backbone

Mathilde H. Lerche, Axel Meissner, Flemming M. Poulsen, and Ole Winneche Sørensen

Department of Chemistry, Carlsberg Laboratory, Gamle Carlsberg Vej 10, DK-2500 Valby, Denmark

Received March 8, 1999; revised May 17, 1999

A set of three improved two-dimensional (2D) NMR methods for measuring one-bond ^{15}N–^{1}H coupling constants in the protein backbone is presented. They are tailored to suit the size of the TROSY effect, i.e., the degree of interference between dipolar and chemical shift anisotropy relaxation mechanisms. The methods edit 2D spectra into two separate subspectra corresponding to the two possible spin states of the coupling partner. Cross talk between the two subspectra is a second order effect in the difference between the actual coupling constants and the one used in setting the pertinent delays of the pulse sequences. This relatively high degree of editing accuracy makes the methods useful for applications to molecules subjected to weak alignment where the one-bond coupling constants are linear combinations of a scalar J and a residual dipolar contribution containing important structural information. A demonstration of the new methods is shown for the ^{15}N-labeled protein chymotrypsin inhibitor 2 in a lipid bicelle mixture.

Key Words: **S^3CT; TROSY; bicelles; residual dipolar coupling constants.**

It has long been known that heteronuclear one-bond J coupling constants between a proton and another directly attached nucleus in a protein backbone contain structural information. Moreover, measurements of these one-bond coupling constants recently became very important when the methods for weak alignment of proteins made residual dipolar coupling constants accessible (*1, 2*).

A convenient way of measuring such coupling constants is by spin-state selective (S^3) techniques (*3–10*), where the two components of doublets or two or four components of two-dimensional (2D) multiplets of I–S two-spin systems are edited into separate subspectra. In particular, two criteria for the choice of pulse sequence are relevant. First of all, it is as always of interest to keep pulse sequences as short as possible. Second, it is necessary that the pulse sequences and thereby the editing into subspectra are relatively insensitive to a distribution in the sizes of the coupling constants to be measured. Otherwise, cross talk between the edited subspectra will occur. That is not a problem if peaks from different sites are well separated but it reduces the accuracy of the measurements in the case of partially overlapping peaks as is typical in 2D protein NMR spectra. For example, one-bond $^{1}J_{NH}$ coupling constants in proteins cover a relatively narrow range but in bicelle solution with a small degree of alignment, variations of about 10–15% around an average value are typical. Finally, it is also an advantage if the data necessary for producing a subspectrum are all generated by the same pulse sequence apart from phase shifts of some pulses.

Techniques within the S^3E category (*4, 5, 9*) have the lowest tolerance of variation in the coupling constants as cross talk occurs to first order in $\Delta J = |J - J_0|$ where J_0 is the value used in setting the pertinent delays of the pulse sequences. This is a disadvantage except for applications involving, e.g., $^{1}J_{NH}$ in isotropic solution (*11*), and it is not outweighed by the S^3E-type elements having a duration of only $(4J)^{-1}$.

Another type of technique is represented by the category S^3CT (*6*) including S^3P (*7*) or IPAP (*10*). These elements have a duration $(2J)^{-1}$, but as cross talk is a second order effect in ΔJ, they are useful for studies in bicelle solutions. Yet another category of technique where cross talk is also a second order effect in ΔJ is represented by the method known under the three acronyms TROSY (*12*), Double S^3CT (*13*), and α,β-HSQC-α,β (*14*). The duration of this element is J^{-1} but it is optimized with respect to transverse relaxation resulting in a sensitivity advantage for large molecules, i.e., when the TROSY effect is large.

It is the purpose of this Communication to present methods for measuring one-bond ^{15}N–^{1}H coupling constants in the protein backbone that are attractive with respect to the criteria of editing accuracy and length of the pulse sequences. Without strict quantitative limits we distinguish three ranges of the TROSY effect for which different experiments are recommended: small, intermediate, and large. We further use the nomenclature of the TROSY and anti-TROSY resonance to refer to the narrow and the broad lines of doublets, respectively. Finally, the line observed when decoupling the other spin is referred to as neutral with respect to the TROSY effect.

1090-7807/99 $30.00

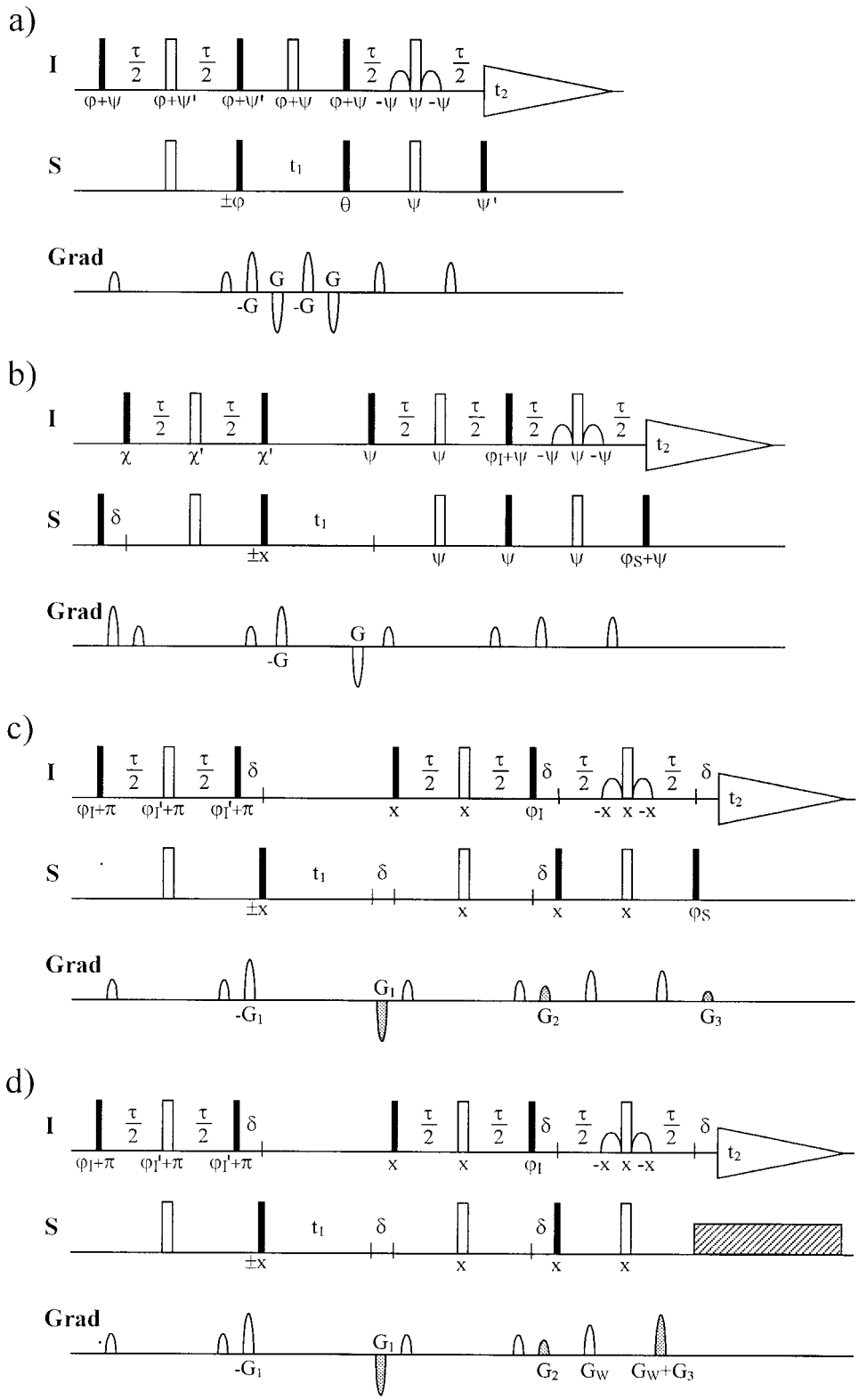

FIG. 1. 2D pulse sequences for measurement of one-bond I–S (^{1}H–^{15}N) coupling constants with editing into α and β subspectra. Except for the first pulse sequence, the ^{1}H (the I spin) carrier frequency must be on-resonance for the water signal. Filled and open bars represent $\pi/2$ and π pulses, respectively. Selective $\pi/2$ Watergate (*15*) pulses are shown as open bell shapes. The phases are indicated below the pulses. $\psi' = \psi + \pi/2$, $\varphi_I' = \varphi_I + \pi/2$, and $\chi' = \chi + \pi/2$ with $\chi = \varphi_I + \psi + \pi$. The prefix $\pm$ on the phase of the $\pi/2(S)$ pulse preceding t_1 indicates an independent high priority two-step phase cycle with opposite receiver phase. All other phase cycles below occur at constant receiver phase. The phases in the initial INEPT transfer are adjusted to return the water magnetization to

In Fig. 1a is shown the 2D S^3CT pulse sequence (*6*) tailored for small TROSY effects. It employs the scheme of Mori *et al.* (*16, 17*) to avoid saturating the water. The S^3CT sequence yields two 2D subspectra with the coupled *I*-spin resonances in the ω_2 dimension corresponding to the *S* spin being in the α and β states, respectively, while the *I*-decoupled *S*-spin chemical shifts are observed in the ω_1 dimension. The pulse sequence is very short, but it requires observation of neutral/anti-TROSY peaks in one of the subspectra limiting its application to molecules with small TROSY effects.

For intermediate TROSY effects a higher sensitivity will be obtained by the pulse sequence outlined in Fig. 1b where so-called semi-TROSY peaks are observed, i.e., TROSY/anti-TROSY and anti-TROSY/TROSY. In other words, in comparison to the method of Fig. 1a, neutral in one of the dimensions is replaced by TROSY for the peak of lowest intensity. The pulse sequence is a special case of Double S^3CT (*13*), while the basic setup is the same as that used by Rance *et al.* (*17*). The required linear combinations of data sets have also been suggested by Andersson *et al.* (*14*).

In systems where large TROSY effects prevail it is unattractive to have anti-TROSY in one of the dimensions. Hence we suggest using the genuine TROSY approach to obtain exclusively the TROSY peak (i.e., TROSY resonance in both dimensions) by the pulse sequence in Fig. 1c for this application. This spectrum must be supplemented by a spectrum having neutral/TROSY or TROSY/neutral peaks. To obtain such peaks either the sequence in Fig. 1a selecting only the TROSY resonances in ω_2 or the sequence in Fig. 1d selecting the TROSY resonances in ω_1 can be used. The price to pay for the improved sensitivity of this approach compared to the one of the semi-TROSY peaks is a reduction in the peak separations to half their values. In particular when the sequence in Fig. 1d with *S*-spin multipulse decoupling during acquisition is used, it is important to record the two subspectra in an interleaved fashion. Otherwise, temperature effects may slightly shift the peaks.

It should be noted that the sequences in Figs. 1c and 1d could also be realized with the setup of Fig. 1b without δ delays if the gradient enhanced heteronuclear echo or antiecho selection improving the water suppression is dispensed with. In the absence of pulse imperfections and the TROSY effect, and ignoring different relaxation during the experiments, all pulse sequences in Fig. 1 exhibit identical sensitivity for the peaks they produce. Furthermore, although not observed in our test spectra of a relative small protein (vide infra), all the experiments in Fig. 1 are susceptible to artifacts caused by different relaxation rates of the various coherences present during the mixing sequences (*17*).

An experimental demonstration of the described methods is shown in Fig. 2 with excerpts from ^{15}N–^{1}H 2D spectra of ^{15}N-labeled chymotrypsin inhibitor 2 (CI2) recorded with the pulse sequences in Fig. 1. The pairs of edited subspectra are for all three methods plotted in plain and dashed contours, respectively. It is clear that the methods presented offer a convenient and sensitive means of measuring one-bond ^{15}N–^{1}H coupling constants in bicelle solution. Figure 3 shows sections taken through three of the peaks in Fig. 2 and underscores the high editing accuracy and excellent tolerance of a distribution of coupling constants.

CI2 was expressed, purified, and ^{15}N-labeled as described previously (*18, 19*). Dimyristoyl-phosphatidylcholine (DMPC) and dihexanoyl-phosphatidylcholine (DHPC) were purchased from Avanti Polar Lipids, Inc. (Alabaster, AL). A DMPC/DHPC stock solution of 18% w/v was prepared with a ratio of 3.3:1. The phospholipids were weighed under argon and dissolved in two steps. First the readily solvable DHPC was dissolved in a buffer solution (10 mM phosphate, pH 6.5, 0.15 mM NaN_3 in 90% H_2O/10% D_2O) that subsequently was added to the DMPC. In order for the DMPC to dissolve completely,

---

the $+z$ axis before acquisition. τ is $(2J_{XH})^{-1}$, and δ is a gradient delay. Apart from the initial purge gradient in (b) and where otherwise indicated, the pulsed field gradients are arranged in self-compensating pairs. The gradients $-G$ and G during the t_1 periods in (a) and (b) are omitted for the first few t_1 increments until the delays are large enough to accommodate them. (a) S^3CT pulse sequence where the phases φ and θ are cycled to create four data sets: A: ($\varphi = x, -x$) recorded both with $\theta = \psi$ and with $\theta = \psi + \pi$, and the same for B: ($\varphi = y, -y$). Appropriate linear combinations yield the pairs of echo/antiecho data sets for the two subspectra: $(A - B)_{\theta=\psi}$ and $(A + B)_{\theta=\psi+\pi}$ are echo and antiecho, respectively, for the right multiplet components while $(A - B)_{\theta=\psi+\pi}$ and $(A + B)_{\theta=\psi}$ are echo and antiecho, respectively, for the left multiplet components. The phase cycle can be extended by cycling ψ in a manner similar to φ resulting in a total of 8 data sets: A: ($\varphi = x, -x, x, -x$; $\psi = x, x, -x, -x$), B: ($\varphi = y, -y, y, -y$; $\psi = x, x, -x, -x$), C: ($\varphi = x, -x, x, -x$; $\psi = y, y, -y, -y$), D: ($\varphi = y, -y, y, -y$; $\psi = y, y, -y, -y$), all for $\theta = \psi$ and for $\theta = \psi + \pi$. The combinations $\{(A - B) - (C - D)\}_{\theta=\psi}$ and $\{(A + B) + (C + D)\}_{\theta=\psi+\pi}$ yield the echo and antiecho parts, respectively, for the right multiplet components. For the left multiplet components, echo and antiecho are obtained by the combinations $\{(A - B) - (C - D)\}_{\theta=\psi+\pi}$ and $\{(A + B) + (C + D)\}_{\theta=\psi}$, respectively. An imperfect π^I pulse during the t_1 period generates artifacts that can be suppressed by an independent ($x, -x$) two-step phase cycle of this pulse at constant receiver phase. (b) Pulse sequences for recording semi-TROSY peaks. The phase ψ is cycled to create two data sets that contain both semi-TROSY resonances of the multiplets for the echo and antiecho pathways, respectively: A: ($\psi = x, -x$) is recorded with ($\varphi_I = y$; $\varphi_S = -y$) and with ($\varphi_I = -y$; $\varphi_S = y$), and the same for B: ($\psi = y, -y$). Then $(A - B)_{\varphi I=y;\ \varphi S=-y}$ and $(A + B)_{\varphi I=-y;\ \varphi S=y}$ are echo and antiecho, respectively, for the subspectrum containing the upper right multiplet components while $(A - B)_{\varphi I=-y;\ \varphi S=y}$ and $(A + B)_{\varphi I=y;\ \varphi S=-y}$ are echo and antiecho, respectively, for the subspectrum containing the lower left multiplet components. (c) TROSY sequence where echo/antiecho selection is achieved by the shaded pulsed field gradients. For ^{1}H and ^{15}N spins the echo is obtained for $\varphi_I = -y$; $\varphi_S = -y$, $G_1 = -7$, $G_2 = 3$, $G_3 = 2$, and antiecho for $\varphi_I = y$; $\varphi_S = y$, $G_1 = -8$, $G_2 = 2$, $G_3 = 3$. (d) TROSY sequence with decoupling in t_2 employing the same phase and gradient settings as in (c). All phase settings in this figure apply for Varian Unity Inova spectrometers; for Bruker instruments the phase of the first π^I pulse must be shifted by $\pi/2$ and φ_I and φ_S inverted in the sequences in (c) and (d) (*13*).

this solution was placed on a shaker at 20°C for 3 days. Dilute bicelle NMR samples were obtained by the addition of buffer to the bicelle stock solution and subsequently adding this dilute bicelle solution to freeze-dried protein. The resulting NMR sample was 1 mM ^{15}N-labeled CI2 in a 4% w/v DMPC:DHPC 3.3:1.

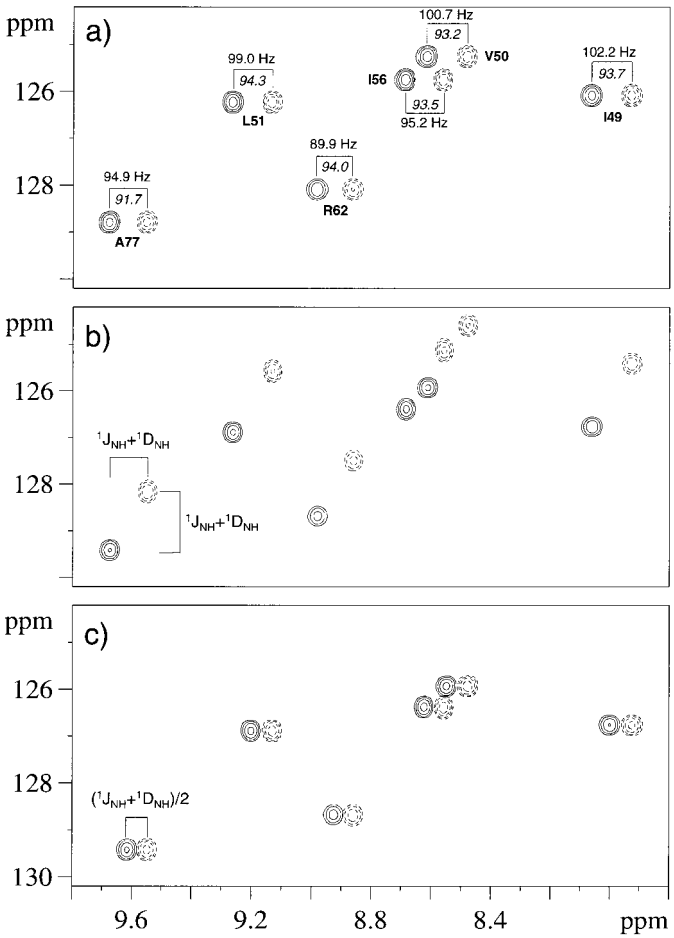

FIG. 2. Excerpts from the 2D S^{3}CT spectrum (pulse sequence in Fig. 1a) (a), the semi-TROSY spectrum (pulse sequence in Fig. 1b) (b), and the TROSY and ω_2-decoupled TROSY spectra recorded with the pulse sequences in Figs. 1c and 1d, respectively (c), of 1 mM ^{15}N-labeled CI2. The protein was dissolved in a 10 mM phosphate, pH 6.5, 0.15 mM NaN_3, 4% DMPC/DHPC 3.3:1 solution of 90% H_2O/10% D_2O and measured at 37°C. The spectra were all recorded on a Varian Unity Inova 750 MHz spectrometer and processed with the Bruker XWINNMR software package after a short C program had made the required linear combinations of data. Parameters applied in all experiments: relaxation delay 1.5 s; $\tau = 5.26$ ms; $\delta = 1.1$ ms; $t_1(\max) = 32.6$ ms; and a total of 32 scans for each set of experiments. Spectral widths of 3900 Hz in the ^{15}N and 12,000 Hz in the ^{1}H dimension were recorded in a data matrix of 256 × 1024 points. The subspectra were combined as described in the legend of Fig. 1. All spectra were zero-filled to 2048 × 4096 points prior to Fourier transformation and cosine window functions were applied in both dimensions. The two edited subspectra (plain and dashed contours) provide the measurement of $^1J_{NH} + {}^1D_{NH}$ in (a) and (b) and of $(^1J_{NH} + {}^1D_{NH})/2$ in (c). The coupling constants indicated are measured from 1D sections like those shown in Fig. 3 with a precision of about ±0.2 Hz. A higher accuracy can be obtained by taking the entire 2D peakshapes into account. The *J* coupling constants written in italic are those measured in isotropic phase.

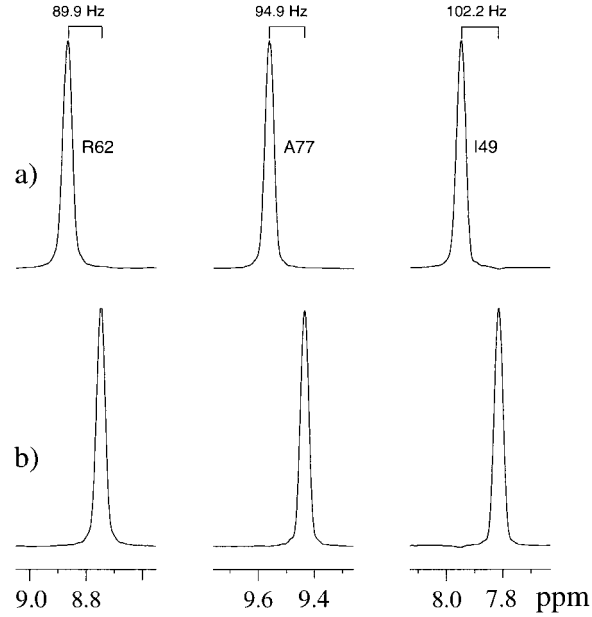

FIG. 3. 1D sections through three representative cross peaks in the edited 2D S^{3}CT subspectra of ^{15}N-labelled CI2 in Fig. 1a; (a) left and (b) right multiplet components, respectively. Note the high editing accuracy resulting in virtually no cross talk between the two subspectra.

In conclusion, we have described a set of three methods for measurement of heteronuclear one-bond coupling constants covering the range of the TROSY effect, i.e., the degree of interference between dipolar and chemical shift anisotropy relaxation mechanisms. The merits of the methods are relatively short pulse sequences and a high degree of editing accuracy that is crucial in applications to proteins or other biomolecules dissolved in bicelles or similar media enforcing a small degree of molecular alignment.

ACKNOWLEDGMENTS

The spectra presented were recorded on the Varian Unity Inova 750 MHz spectrometer of the Danish Instrument Center for NMR Spectroscopy of Biological Macromolecules at Carlsberg Laboratory. We thank Kim Vilbour Andersen for the ^{15}N chemical shift assignments of apo-CI2 and Pia Skovgaard for skillful technical assistance. MHL and FMP acknowledge support from the Danish Biotechnology Initiative funded by the Danish Natural Science Research Council.

REFERENCES

1. J. R. Tolman, J. M. Flanagan, M. A. Kennedy, and J. H. Prestegard, *Proc. Natl. Acad. Sci. USA* **92,** 9279–9283 (1995).
2. N. Tjandra and A. Bax, *Science* **278,** 1111–1114 (1997).
3. N. C. Nielsen, H. Thøgersen, and O. W. Sørensen, *J. Chem. Phys.* **105,** 3962–3968 (1996).
4. A. Meissner, J. Ø. Duus, and O. W. Sørensen, *J. Magn. Reson.* **128,** 92–97 (1997).
5. A. Meissner, J. Ø. Duus, and O. W. Sørensen, *J. Biomol. NMR* **10,** 89–94 (1997).

6. M. D. Sørensen, A. Meissner, and O. W. Sørensen, *J. Biomol. NMR* **10,** 181–186 (1997).
7. A. Meissner, T. Schulte-Herbrüggen, and O. W. Sørensen, *J. Am. Chem. Soc.* **120,** 3803–3804 (1998).
8. J. Briand and O. W. Sørensen, *J. Magn. Reson.* **135,** 44–49 (1998).
9. P. Andersson, K. Nordstrand, M. Sunnerhagen, E. Liepinsh, I. Turovskis, and G. Otting, *J. Biomol. NMR* **11,** 445–450 (1998).
10. M. Ottiger, F. Delaglio, and A. Bax, *J. Magn. Reson.* **131,** 373–378 (1998).
11. A. Meissner, T. Schulte-Herbrüggen, and O. W. Sørensen, *J. Am. Chem. Soc.* **120,** 7989–7990 (1998).
12. K. Pervushin, R. Riek, G. Wider, and K. Wüthrich, *Proc. Natl. Acad. Sci. U.S.A.* **94,** 12366–12371 (1997).
13. A. Meissner, T. Schulte-Herbrüggen, J. Briand, and O. W. Sørensen, *Mol. Phys.* **95,** 1137–1142 (1998).
14. P. Anderson, A. Annila, and G. Otting, *J. Magn. Reson.* **133,** 364–367 (1998).
15. M. Piotto, V. Saudek, and V. Sklenar, *J. Biomol. NMR* **2,** 661–665 (1992).
16. S. Mori, C. Abeygunawardana, M. O. Johnson, and P. C. M. van Zijl, *J. Magn. Reson.* **108,** 94–98 (1995).
17. M. Rance, J. P. Loria, and A. G. Palmer III, *J. Magn. Reson.* **136,** 92–101 (1999).
18. P. Osmark, P. Sørensen and F. M. Poulsen, *Biochemistry* **32,** 11007–11014 (1993).
19. J. C. Madsen, O. W. Sørensen, P. Sørensen and F. M. Poulsen, *J. Biomol. NMR* **3,** 239–244 (1993).